Role of Clay-humus Complexes in Soil Organic Carbon Stabilization Across Paddy Soils in Diverse Indian Soil Orders

Kavitha P Jadhav [a], Nayan Ahmed [b*], Tapan Jyoti Purakayastha [b], Debasis Golui [b], Ruma Das [c], Mahesh Chand Meena [b], Manoj Shrivastava [d], Rajeev Ranjan [e] and Pooja Tamuk [b]

[a] Division of Soil Science, ICAR-Indian Institute of Soil and Water Conservation, Research Centre, Ballari, Karnataka, India.
[b] Division of Soil Science and Agricultural Chemistry, ICAR-Indian Agricultural Research Institute, New Delhi, India.
[c] ICAR- National Bureau of Soil Survey and Land Use Planning, Regional Center, Kolkata, West Bengal, India.
[d] Division of Environment Science, ICAR-Indian Agricultural Research Institute, New Delhi, India.
[e] Division of Agricultural Physics, ICAR-Indian Agricultural Research Institute, New Delhi, India.

Authors' contributions

This work was carried out in collaboration among all authors. All authors read and approved the final manuscript.

Original Research Article

_____

Corresponding author: E-mail: nayan.ahmed@gmail.com;

ABSTRACT

Aims: This study investigates the mechanisms of soil organic carbon (SOC) stabilization within clay-humus complexes across diverse soil orders in Indian paddy soils. By employing FTIR spectroscopy and NaOCl oxidation, it examines how different clay mineral compositions, such as smectite-rich Vertisols, influence SOC stability.

Place and Duration of Study: Soil samples were collected from paddy-growing regions in India-Entisol from Nadia (West Bengal), Inceptisol from Sonipat (Haryana), Vertisol from Belgaum (Karnataka), and Alfisol from Davanagere (Karnataka), between June 2019 and July 2020.

Methodology: Soil samples were collected from paddy-growing regions across four Indian soil orders: Entisol, Inceptisol, Vertisol, and Alfisol. SOC stabilization was analyzed through X-ray diffraction (XRD) for mineral composition, total and NaOCl-resistant carbon measurements, and FTIR spectroscopy to characterize functional groups in humic acids and clay-humus complexes.

Results: The study found that Vertisol soils, with higher smectite content, showed the highest level of total and stable carbon, while Alfisols, dominated by kaolinite, exhibited lower stability. FTIR analysis indicated strong aromaticity in Vertisol's humic acid, suggesting enhanced stability through complex mineral interactions

Conclusion: This research highlights the crucial role of soil mineralogy in SOC stabilization, with significant implications for carbon sequestration strategies in Indian paddy soils. These findings could support targeted soil management practices for enhancing SOC retention and promoting sustainable agriculture.

1. INTRODUCTION

Soil organic carbon (SOC) is crucial for soil quality and ecosystem health, serving as a key indicator of soil vitality. Its depletion adversely affects soil aggregation, stability, water retention, fertility, and biological activity (Rashid et al., 2022; Kundu et al., 2022). The presence and stability of SOC are central to maintaining these vital soil functions, contributing to soil structure and productivity (Lal, 2021). SOC dynamics are influenced by management practices, soil type, and climate. SOC stabilization occurs through physical protection, primarily via soil aggregates, which encase SOC within the aggregates, reducing its exposure to microbial decomposition and environmental loss (Das et al., 2018). Chemical processes (Lutzow et al., 2009), such as adsorption of SOC onto mineral surfaces or aqueous complexation of dissolved organics with mineral weathering products, also play a major role in its stabilization. The interaction between SOC and clay minerals, forming clay-humus complexes, is particularly significant, as these complexes provide long-term protection for SOC by creating stable microenvironments that shield organic matter from microbial and chemical breakdown (Singh et al., 2017). Chemical reactions associated with the breakdown of complex organic compounds may potentially contribute to the stability of particular SOC compounds. Chemical weathering reactions cause changes in soil mineralogy over time (Lawrence et al., 2015), influencing other soil parameters that affect SOC stability as a result of the evolution of soil mineralogy. Because different clay minerals form distinct clay-humus complexes, the mineralogy of the soil directly impacts the effectiveness of physical and chemical mechanisms in protecting SOC (Kumari and Mohan, 2021). As a result, the relative relevance of various mechanisms of soil organic matter (SOM) physical and chemical protection changes over time, depending on the dominant clay minerals and their interactions with organic matter.

For decades, it has been well known that SOM is primarily linked to the mineral structure, with varying degrees of stability facilitated by hydrogen bonds, van der Waals bonds, ligand exchange, and polyvalent cation bridging (Stoner et al., 2023; Mabagala, 2022). These interactions serve to protect SOM from degradation by various agents, including microbial activity and environmental factors (Singh et al., 2023). The degree to which carbon (C) is protected from decomposition is largely determined by the mineral composition of clay particles (Schweizer et al., 2021; Yang et al., 2021). Clay minerals, particularly through their interaction with organic matter to form clay-humus complexes, not only stabilize SOM but also reduce the risk of SOM loss due to respiration, erosion, and leaching (Sakar et al., 2018). The type of phyllosilicate clays present in the soil

significantly influences the stabilization and subsequent accumulation of organic carbon (OC). Clay-humus complexes are especially important for SOC stabilization, as they provide a stable microenvironment that protects organic matter from microbial decomposition (Naresh et al., 2018). Due to their charge characteristics, small particle size, and large surface area, are crucial for organic matter stabilization. However, the extent of protection provided by these complexes varies, as different clay minerals have distinct specific surface areas and charge properties (Sakar et al., 2018). Because the dominant clay minerals in different soil orders vary, the same management practices may have differing effects on carbon stabilization by clay-humus complexes across soils (Kumari and Mohan, 2021. There are various mechanisms involved in the stabilization of OC and different techniques are utilized to isolate the old and chemically resistant OC component from soils. The use of sodium hypochlorite (NaOCl) to create a chemically resistant SOM fraction attached to mineral surfaces (Bottone et al. 2022). The OC that is resistant to NaOCl oxidation is referred to as a recalcitrant or stable OC (Jagadamma et al. 2010). Following NaOCl treatment, we can extract mineral-protected OC by the dissolution of the mineral phase. We hypothesized that OC left after the NaOCl treatment was largely stabilized by its inherent chemical composition, thus representing recalcitrant or stable OC in soil.

Previous research has highlighted the critical role of long-term fertilization and manuring with diverse organics in enhancing carbon stability within the clay-humus complex across soils with varying clay mineralogy. Distinct clay minerals and bridging cations dominate different soil orders, affecting organic carbon (OC) stabilization to varying extents (Ahmed et al., 2002). A recent study by Kumar et al. (2022) examined the influence of integrated farmyard manure, green manure, and biofertilizers on soil carbon stability in Inceptisols under rice-wheat rotation in semi-arid, sub-tropical India. While conservation tillage especially with residue conservation has demonstrated positive effects on soil composition, water-stable aggregates, and microbial biomass in Inceptisols under rice-wheat cropping systems (Naresh et al., 2018), a crucial gap remains in our understanding of OC dynamics in paddy soils (Kaushal et al., 2023). These flooded or submerged soils, widely used for rice cultivation, serve as both a source and sink of carbon, with their carbon status influenced by regional mineralogy and specific management practices.In order to unravel the

mechanisms underlying OC association with mineral surfaces and its long-term stability, particularly in paddy soils, it is essential to obtain comprehensive insights into the formation and properties of humic substances, such as humic acid (HA). Understanding these interactions at a detailed level can reveal the complex processes of clay-humus complex formation and OC protection. Such insights are essential for developing soil management practices that enhance carbon sequestration, especially in agroecosystems where paddy soils play a significant role in global carbon cycling.

The novelty of this study lies in its innovative combination of FTIR spectroscopy with NaOCl oxidation to examine clay-humus interactions in the stabilization of SOC. FTIR spectroscopy allows for the detailed identification of chemical bonds and functional groups in organic matter, while NaOCl oxidation isolates chemically resistant, recalcitrant carbon by removing more labile organic matter. This dual-method approach provides a comprehensive view of how different clay minerals interact with humus stable organic matter to stabilize SOC, a perspective not widely explored in prior studies. Additionally, by applying this methodology to various Indian paddy soils, the study addresses a significant research gap, offering new insights into the role of clay mineralogy in SOC stability within these specific soils. The findings not only contribute to a better understanding of SOC dynamics but also have practical implications for targeted soil management and carbon sequestration strategies, supporting sustainable agriculture and environmental conservation efforts.

2. MATERIALS AND METHODS

To address the above objectives, HA, clay and clay-humus complexes were extracted from diverse soil orders and the NaOCl-resistant carbon in the clay-humus complexes was estimated. FTIR spectroscopy was used to characterize the functional groups of HA, clay and clay-humus complexes by analyzing infrared absorption peaks, focusing on carbon stabilization in different soil orders.

2.1 Location and Soil Sampling

Soil samples were collected from diverse paddy-growing states in India, representing various soil orders Entisol from Nadia, West Bengal; Inceptisol from Sonipat, Haryana;Vertisol from Belgaum, Karnataka; and Alfisol from Davanagere,

Karnataka (Fig.1). Replicated composite soil samples were collected at a depth of 0-30 cm.

Soil samples were dried in the air, ground by a wooden pestle and mortar, and passed through a 2 mm sieve before analysis. Vertisol is clay-rich soil found in Belgaum, Karnataka, with high fertility and swelling/shrinking properties. Alfisol is moderately leached, fertile soils found in Davangere, Karnataka. Inceptisol is the young soil with minimal horizon development, found in Sonipat, Haryana, and suitable for agriculture. Entisol is the youngest soil with little horizon development, found in Nadia, West Bengal, with lower fertility compared to other orders (Table 1).

2.2 Clay Mineralogy Study

Clay mineralogy of the collected soil was performed by separating the clay particles (< 2 μm) following the procedure outlined by Jackson (1985). The clay samples underwent four different treatments: (i) magnesium (Mg) saturated and air-dried (Mg-air), (ii) Mg-saturated and glycerol solvated (Mg-gly), (iii) potassium (K) saturated and air-dried (K-air), and (iv) K saturated and heated at 550 °C for 2 hours (K-550). The X-ray diffractograms of the treated clay samples were recorded using a Philips diffractometer (X-ray generator: PW-1729, diffractometer control: PW-1710, Philips, Holland) utilizing Ni-filtered Cu-Kα radiation at a scanning speed of 1.5° 2θ min-1.

2.3 Clay-Humus Complex Analysis

The clay-humus complex was separated following Datta et al. (2015): 20 g of soil was mixed with 200 ml distilled water, stirred for 15 minutes, and dispersed with an ultrasonic vibrator. The suspension was left to settle, and the upper layer containing clay-humus (<2 μm) was siphoned off. This process was repeated until clear supernatant. The clay-humus complex extracted was pooled, concentrated by centrifugation, and freeze-dried. Total carbon content was determined using a CHNS analyzer. NaOCl treatment removed labile organic matter, with NaOCl-resistant C measured as stable carbon, and labile carbon calculated as the difference from total carbon.

2.4 Extraction and Characterization of Humic Acid (HA)

HAs were extracted from soils following the International Humic Substance Society (IHSS) method. Air-dried soil was acidified to pH 1-2 with 1 M HCl, shaken, and the supernatant removed for fulvic acid isolation. The soil residue was neutralized, treated with 0.1 M NaOH, and left to settle. The supernatant was acidified to pH 1 to precipitate HA, which was then separated by centrifugation, re-dissolved in 0.1 M KOH, and re-precipitated with 6 M HCl. The precipitate was treated with 0.1 M HCl/0.3 M HF to reduce ash, dialyzed, and freeze-dried. Elemental
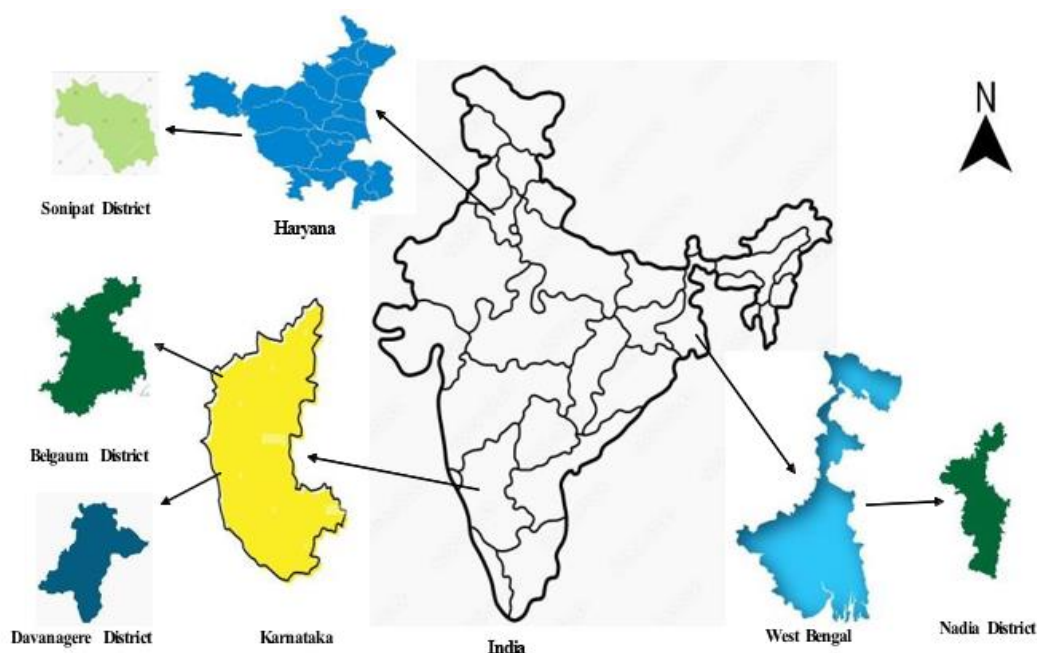

Fig. 1. Map showing soil sample collection sites across paddy-growing regions in India

analysis and functional group assessments were conducted using CHNS analysis and standard methods (Stevenson, 1994; Schnitzer, 1965).

2.5 FTIR Spectroscopy

The stabilization of C was probed by spectroscopic analysis of HA, clay and clay-humus complexes isolated from different soil orders. Samples were vacuum dried, ground, and characterized using a Bruker (Alpha) instrument. FTIR spectra (600-4000 cm-1) of HA, clay, and clay-humus complexes were recorded on KBr-pressed tablets.

2.6 Statistical Analysis

Data were statistically analyzed using two-way Analysis of Variance (ANOVA) in OPSTAT online statistical package (Hisar Agricultural University). Duncan's Multiple Range Test (DMRT) was applied for comparisons of treatment means, allowing for precise identification of statistically significant variations in soil properties and organic matter dynamics. The analyses were performed using SPSS software, version 10.0 for Windows, ensuring reliable and rigorous evaluation of the experimental data. This comprehensive methodology ensures a robust investigation into soil properties and organic matter dynamics across diverse soil orders.

3. RESULTS

3.1 Clay Mineralogy of Soils

XRD analysis of clay samples from different soils provides critical mineral insights (Fig. 2). In Vertisol from Belgaum, Karnataka, a basal reflection at 6.1° 2θ (d 1.43 nm) shifted to 4.9° 2θ (d 1.78 nm) after glycerol treatment, indicating smectite. Peaks at 8.5-9° 2θ (d 1.02-0.97 nm)

suggest mica and illite, while K-saturated samples showed a kaolinite peak at 12.5° 2θ (d 0.70 nm), disappearing at 550°C. In Alfisol, kaolinite was evident across treatments, disappearing at 550°C, and Mg-treated samples showed vermiculite with a shift after glycerol treatment, while K-air samples retained a chlorite peak at 10° 2θ (d 0.87 nm) after heating. For Inceptisol from Sonipat, Haryana, the presence of smectite was confirmed by a shift from 6.1° to 4.9° 2θ after glycerol treatment, with stable illite peaks at 8.8° 2θ (d 0.98 nm). Kaolinite appeared at 12.1° 2θ (d 0.72 nm), disappearing at 550°C. In Entisol from West Bengal, Mg-air samples showed a stable chlorite peak at 6.2° 2θ, with HIC formation at 7.5° 2θ after heating. Persistent peaks at 8.8-8.9° 2θ confirmed illite, while kaolinite was indicated by a 12° 2θ peak, absent at 550°C.

3.2 Total and NaOCl-Resistant C in Clay-Humus Complexes

The total C content within clay-humus complexes exhibited considerable variability across different soil orders (Table 2), ranging from 2.19 to 8.12 g kg-1. The highest recorded total C content (8.12 g kg-1) was observed in Vertisol, followed by Inceptisol (5.41 g kg-1) and Entisol (3.24 g kg-1), while the lowest was in Alfisol (2.19 g kg-1). Chemically resistant SOM fractions bound to mineral surfaces were obtained through the use of NaOCl method. OC that resists oxidation by NaOCl is considered stable C. The NaOCl-resistant C exhibited significant variation among different soil orders. Vertisol displayed the highest stable C content (3.96 g kg-1), followed by Inceptisol (1.54 g kg-1), with the lowest observed in Alfisol (0.22 g kg-1). The difference between the total C and NaOCl-resistant C values represents the labile C fraction, which ranged from 0.19% in Alfisol to 0.41% in Vertisol.

Table 1. Initial properties of soil collected from diverse soil orders of India

Soil orders	Vertisol	Alfisol	Inceptisol	Entisol
Location	Belguam, Karnataka	Davangere, Karnataka	Sonipat, Haryana	Nadia, west Bengal
Climate	Tropical	Tropical	Humid subtropical	Humid Tropical
pH	7.89	6.86	7.84	6.64
OC (g/kg)	9.91	6.82	9.21	3.76
CEC (Cmol(p$^+$)/kg)	28.44	12.27	12.36	8.67
Sand (%)	10.11	55.84	40.48	40.43
Silt (%)	20.09	8.27	25.98	23.09
Clay (%)	70.1	35.9	33.54	36.28
Texture	Clay	Sandy clay loam	Clay loam	Clay loam
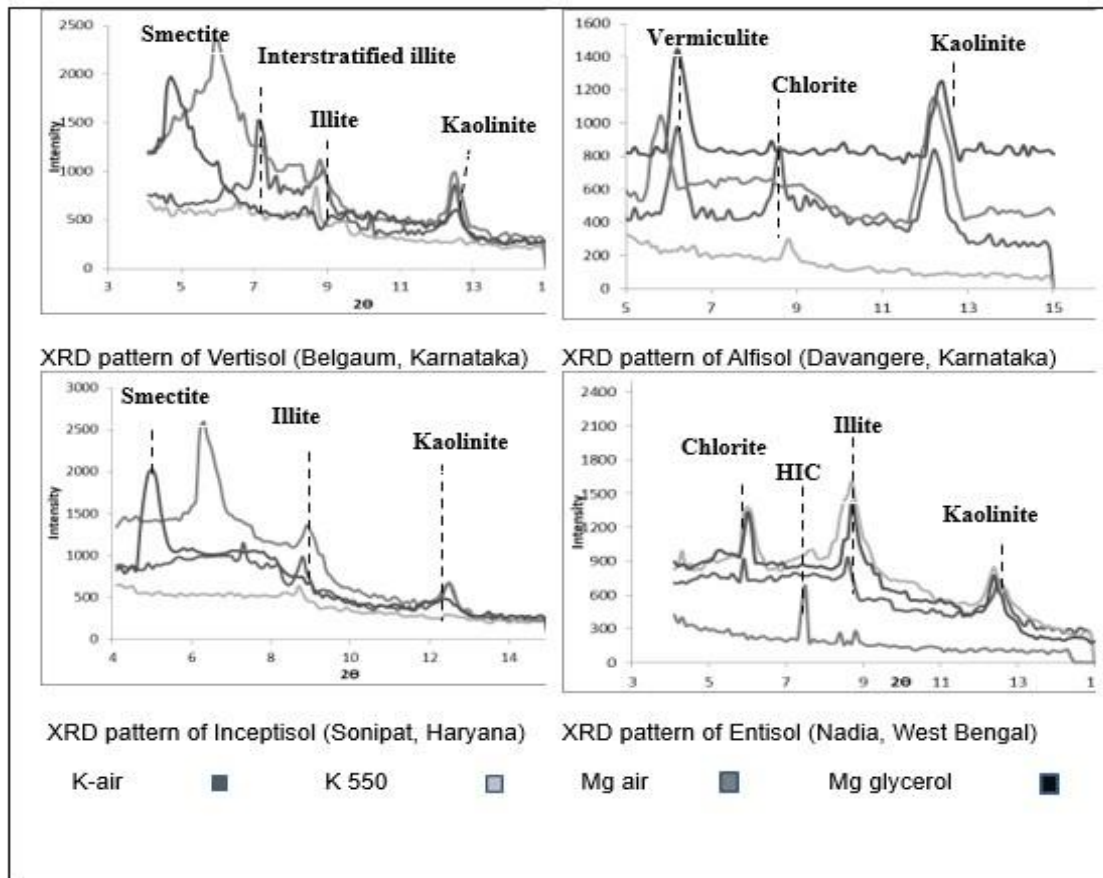
Fig. 2. Identification of clay minerals in diverse soil orders of India by X-ray diffraction method

Table 2. Total C and NaOCl-C content in clay humus complexes of diverse soil orders

Soil Orders	Total C (g kg⁻¹)	NaOCl-C (g kg⁻¹)	Labile C (%)
Vertisol	8.12[a]	3.96[a]	0.41[a]
Alfisol	2.19[d]	0.22 [d]	0.19[d]
Inceptisol	5.41[b]	1.54[b]	0.38[b]
Entisol	3.24[c]	0.89[c]	0.21[c]

Table 3. Elemental composition of humic acids isolated from diverse soil orders

Soil orders	C (%)	H (%)	N (%)	S (%)	O (%)
Vertisol	57.39[a]	4.55[a]	4.64[a]	0.45[a]	33.07[d]
Alfisol	53.77[c]	3.85[c]	3.67[c]	0.30[c]	38.41[b]
Inceptisol	54.49[b]	4.05[b]	4.01[b]	0.37[b]	36.93[c]
Entisol	53.66[d]	3.50[d]	3.25[d]	0.19[d]	39.90[a]

3.3 Chemical Characterization of Humic Acids

Table 3 presents the elemental composition of HA isolated from different soil orders, revealing that HAs from all soil types exhibit a higher carbon content and lower oxygen content, which are indicative of typical HA characteristics. The C content ranged from 53.66 to 57.39 percent, with significantly higher value observed in Vertisol. The sequence of carbon content across soil orders is as follows: Vertisol > Inceptisol >

Alfisol> Entisol. Additionally, hydrogen, nitrogen, and sulfur content were significantly higher in Vertisol, followed by Inceptisol, and were lowest in Entisol.

The data on functional groups presented in Table 4 reveal variations in the total acidity (meq g-1) of HAs across different soil orders. The total acidity ranged from 3.80 in Entisol to 6.90 meq. g-1, in Vertisol. Notably, Vertisol exhibited significantly higher total acidity (6.90 meq. g-1), followed by Inceptisol (6.33 meq. g-1) and Alfisol (5.96 meq. g-1), while Entisol recorded significantly lower total acidity (3.80 meq g-1).

A similar trend was observed in the case of carboxyl and phenolic groups, with Vertisol featuring significantly higher values and Entisol displaying the lowest values. The degree of aliphaticity or aromaticity in humic substances, as indicated by the E4/E6 ratio i.e. absorbance at wavelengths of 465 nm and 665 nm, exhibited a significantly lower value in Vertisol, followed by Inceptisol, whereas the highest values were observed in Entisol, followed by Alfisol. The E4/E6 ratio of less than 5 suggests that the HA fraction in these soils possesses a higher degree of condensation of aromatic humic compounds,

low acidity, and a high molecular weight. Notably, the higher E4/E6 ratio of 4.56 in Entisol indicates that its HA is less condensed compared to HAs from other soil orders.

3.4 FTIR Spectra of Humic Acids

The FTIR spectra depicted in Fig.3 showcase the distinctive characteristics of HAs isolated from diverse soil orders. The assignments of various absorption peaks in different soil ordes are comprehensively detailed in Table 5. Notably, key features are observed in specific spectral regions, including the H-bond OH stretching in the range of 3850-3620 cm⁻¹, aliphatic C-H stretching at 2940-2900 cm⁻¹, and triple bond C≡N and C≡C vibrations spanning 2398-2310 cm⁻¹. Furthermore, significant peaks are identified at 1698-1691 cm⁻¹, indicative of COOH vibrations, and at 1607-1623 cm⁻¹, representing aromatic C=C and C=O stretching in amide, ketone, and quinone groups. The spectral region of 1517-1506 cm⁻¹ is associated with COO- symmetric stretching, N-H bending, and C=N stretching. Additionally, the presence of C-O stretching and OH deformation of COOH, along with C-O stretching of aryl ethers, is manifested in the range of 1220-1205 cm⁻¹.

a. Vertisol humic acid

b. Alfisol humic acid

c. Inceptisol humic acid
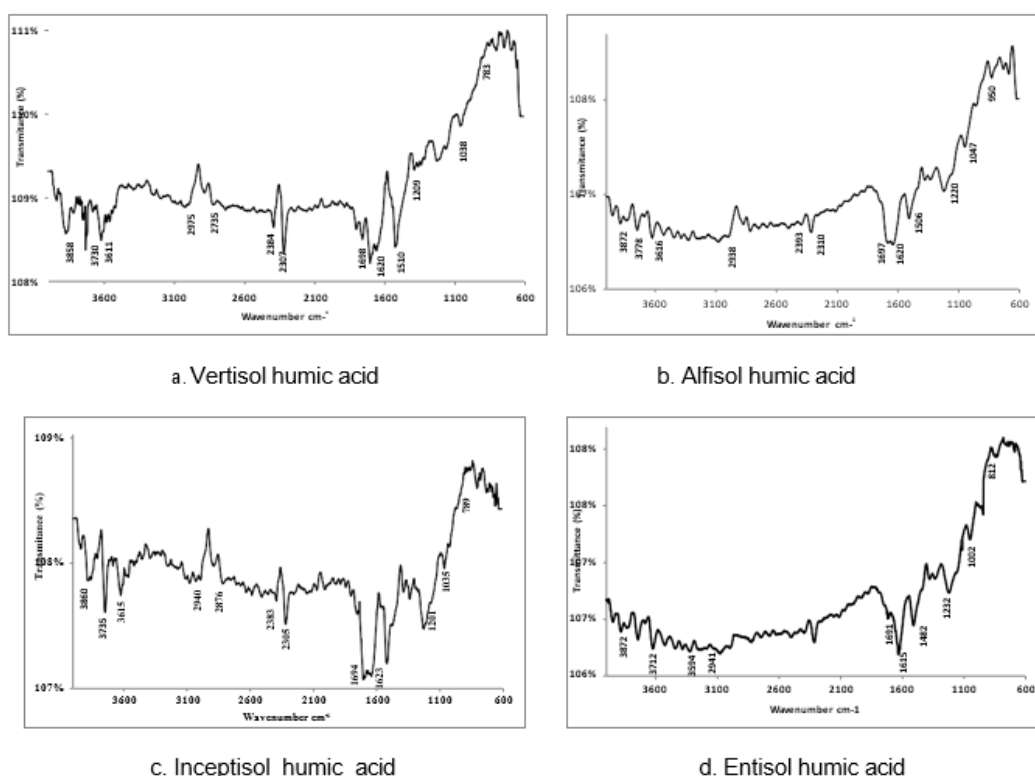
d. Entisol humic acid

Fig. 3. FTIR spectra of humic acids isolated from soils of diverse soil orders of India

Table 4. Acidic functional groups, total acidity and E4/E6 ratios of humic acids

Soil orders	Total acidity (meq. g-1)	Carboxyl group (meq. g-1)	Phenolic-OH (meq. g-1)	E4/E6 ratio
Vertisol	6.90[a]	3.85[a]	3.05[a]	3.13[d]
Alfisol	5.96[c]	3.49[c]	2.03[c]	3.96[b]
Inceptisol	6.33[b]	3.74[b]	2.26[b]	3.59[c]
Entisol	3.80[d]	2.40[d]	1.40[d]	4.56[a]

Moreover, distinctive peaks at 1030-950 cm^{-1} are attributed to C-O stretching of polysaccharides and Si-O vibrations arising from silicate impurities. Lastly, aliphatic CH2 chains are identified in the spectral range of 750-790 cm^{-1}. This detailed analysis provides insights into the molecular composition and functional groups present in HAs from various soil orders, facilitating a comprehensive understanding of their structural characteristics.

The FTIR spectra of HAs derived from distinct soil orders exhibit common major absorption peaks with minor variations in their relative intensities. A notable divergence is observed in the spectral features, particularly in the Vertisol and Inceptisol samples, where broad and sharp absorption peaks corresponding to aromatic C-C and strong H-bonded C-O stretching of conjugated ketones (1620-1615 cm^{-1}) are prominent. In contrast, the Entisol and Alfisol spectra reveal distinct and robust COOH vibrations at 1698-1691 cm^{-1}.

The 3850 to 3420 cm^{-1} region in Vertisol and Inceptisol spectra displays broad absorption peaks attributed to H-bonded OH groups, which are comparatively reduced and weaker in the case of Entisol and Alfisol. Notably, the absorption associated with aliphatic C-H stretching (2940-2900 cm^{-1}) varies significantly, being pronounced in Vertisol and Inceptisol but less prominent in Entisol and Alfisol. Common absorption peaks in the regions 1517-1506 cm^{-1} attributed to COO- symmetric stretching, N-H bending and C=N stretching, at 1220-1205 cm^{-1} attributed to C-O stretching and OH deformation of COOH, around 1030-950 cm^{-1} attributed to C-O stretching of polysaccharide and Si-O vibrations from silicate impurities and around 790-750 cm^{-1} attributed to aliphatic CH2 chains are discernible in the FTIR spectra of Vertisol, Inceptisol, Entisol, and Alfisol.

3.5 FTIR Spectra of Clay

Fig. 4 displays the FTIR spectra of clays extracted from diverse soil orders, portraying typical infrared signatures representative of clay minerals. The assignments of various absorption peaks of different soil orders are comprehensively detailed in Table 6. The observed spectra exhibit distinctive features encapsulating three primary regions inherent to clay compositions. Firstly, the stretching and bending vibrations of the inner surface hydroxyl (OH) groups are discernible in the spectral range of 3700 to 3400 cm^{-1}. Secondly, the stretching and bending vibrations associated with the Si-O groups manifest within the region spanning 1000 to 936 cm^{-1}. This region provides insights into the structural characteristics of the clay minerals, particularly in relation to the silicon-oxygen bonding within their lattice framework. Thirdly, the Si-O-M (M = Al, Mg, etc.) vibrations are evident in the spectral range extending from 800 to 600 cm^{-1}. These vibrations elucidate the interactions involving silicon and oxygen with additional elements such as aluminum (Al) or magnesium (Mg), contributing to the overall composition and stability of the clay minerals. The collective analysis of these three prominent regions in the FTIR spectra allows for a comprehensive understanding of the molecular structure and bonding interactions present in clays derived from varying soil orders.

The FTIR spectra of clays from Vertisol, Inceptisol, and Entisol show two distinct absorption peaks at 3620 and 3697 cm^{-1} in the O-H stretching region, indicating the presence of smectite clay minerals. The stronger intensity of the 3620 cm^{-1} band compared to the 3697 cm^{-1} peak suggests a dominance of 2:1 type clay minerals. Additional peaks at 3425 cm^{-1} and 1630 cm^{-1} further confirm the presence of smectite.

The unique pattern in the Alfisol IR spectra is characterized by four distinct peaks at 3652, 3671, 3694, and 3620 cm^{-1}. These peaks are attributed to vibrations of surface and inner hydroxyl groups, signifying kaolinite as the major clay mineral in Alfisol. Peaks in the range of 1694-1643 cm^{-1} correspond to strong H-O-H

bonds of absorbed water, highlighting the presence of hydrated phyllosilicate minerals such as chlorite, illite, and smectite in Vertisol, Inceptisol, and Entisol. In contrast, in Alfisol, a strong hydrogen-bonded O-H group is observed, indicating the predominance of kaolinite-rich minerals. The stretching and bending vibrations of the Si-O group, within the range of 1000 to 936 c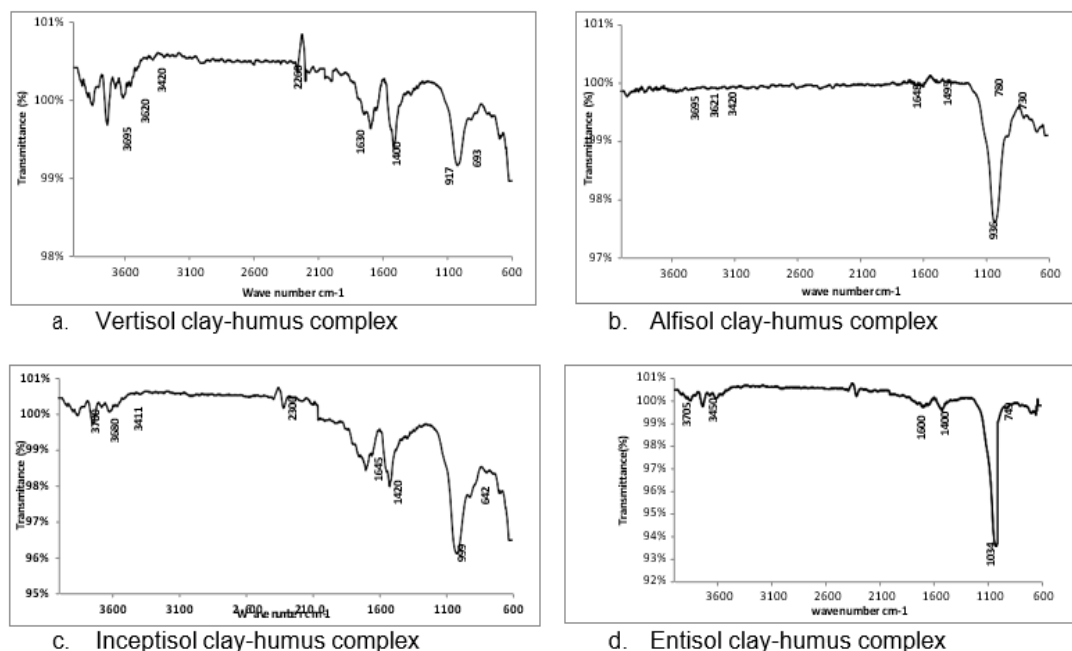m^{-1}, reveal intense Si-O peaks at 1060 and 1007 cm^{-1} for Inceptisol and Entisol, respectively. Additionally, a shoulder peak arising from the Al-OH-Al bending vibration is evident around 909 to 936 cm^{-1} for smectite, illite, and kaolinite, prominently visible in Vertisol and Alfisol, while appearing weakly in Entisol and Inceptisol. This detailed analysis provides insights into the mineralogical composition and structural characteristics of clays across diverse soil orders.

Table 5. Summary of stretching vibrations of various functional groups present in humic acids of different soil orders

Assignment (FTIR peaks in cm^{-1})	Vertisol	Alfisol	Inceptisol	Entisol
Free OH vibration of residual clay mineral or amine (N-H)	3858,3730	3778,3616	3860, 3735,3615	3872, 3594
Aliphatic C-H stretching	2975,2735	2938	2940,2874	2941
Triple bond C≡N and C≡C	2384,2307	2310	2383	
COOH vibrations	1698	1697	1694	1691
Aromatic C-C, strongly H-bonded C-O of conjugated ketones	1620	1620	1623	1615
COO⁻ symmetric stretching, N-H bending, C=N stretching (amide II band)	1510	1506	1509	1482
C-O stretching and OH deformation of COOH, C-O stretching of aryl ethers	1208	1220	1201	1232
C-O stretching of polysaccharide and Si-O of silicates impurities	1038	1047	1035	1002
Aliphatic CH2 chains	783	950	789	812

a. Vertisol clay

b. Alfisol clay

c. Inceptisol clay

d. Entisol clay
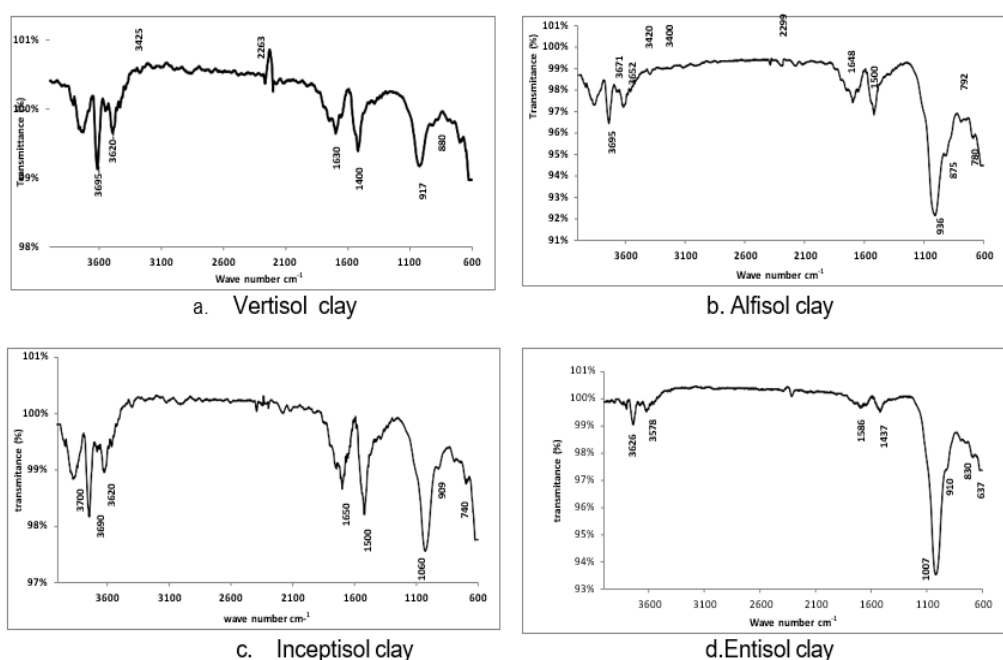
Fig. 4. FTIR spectra of clay isolated from soils of diverse soil orders of India

a. Vertisol clay-humus complex

b. Alfisol clay-humus complex

c. Inceptisol clay-humus complex

d. Entisol clay-humus complex

Fig. 5. FTIR spectra of clay-humus complexes isolated from soils of diverse soil orders of India

Table 6. FTIR spectral features and mineralogical characteristics of clays from different soil orders

Soil Order	Notable Absorption Peaks	Mineral Insights	Key Features in FTIR Spectra
Vertisol	Peaks at 3620 and 3697 cm^{-1} (O-H stretching) Si-O peaks at 1060 cm^{-1} (Si-O stretching) Peak at 909-936 cm^{-1} (Al-OH-Al bending)	Smectite as a major component, indicated by sharp O-H peaks at 3620 cm^{-1}. Hydrated phyllosilicates such as chlorite, illite, and smectite	Presence of smectite, hydrated phyllosilicates
Alfisol	Peaks at 3425 cm^{-1} (O-H stretching) Peaks at 3652, 3671, 3694, 3620 cm^{-1} (O-H stretching). 1694-1643 cm^{-1} (H-O-H bending) Si-O peaks at 1007 cm^{-1}	Predominance of kaolinite with multiple O-H stretching peaks at 3652-3620 cm^{-1}. Smectite also present with Si-O peaks at 1007 cm^{-1}. Hydrated phyllosilicates (chlorite, illite) shown by 1694-1643 cm^{-1} peaks.	Kaolinite with smectite features
Inceptisol	Peaks at 3620 cm^{-1} (O-H stretching). Si-O peak at 1060 cm^{-1} Al-OH-Al bending around 909-936 cm^{-1}	Presence of smectite with a strong O-H peak at 3620 cm^{-1}. Illite confirmed by 1060 cm^{-1} Si-O stretching and 909-936 cm^{-1} Al-OH-Al bending.	Smectite and illite components
Entisol	Peaks at 3620 and 3697 cm^{-1} (O-H stretching) Si-O peak at 1007 cm^{-1} 909-936 cm^{-1} (Al-OH-Al bending)	Smectite present with distinct O-H peaks at 3620 cm^{-1}. Illite indicated by Si-O at 1007 cm^{-1} and Al-OH-Al bending. Kaolinite presence supported by the absence of O-H group peaks in K-550 treatment.	Smectite, illite, and kaolinite

Table 7. FTIR spectral peaks and complexation characteristics of clay-humus complex across different soil orders

Soil Order	Key FTIR Peaks in Clay-Humus Complex (cm^{-1})	Complexation Characteristics	Notable Differences
Vertisol	3800-3000 (O-H stretch); 2300, 2260, 2290, 1500, 1400 (polymerization bands); 1648-1630 (H-O-H bond)	Strong attenuation in 3800-3000 cm^{-1} region, polymerization with HA, reduced intensity in 1648-1630 cm^{-1}	High complexation between clay minerals and HA; significant shift in functional groups
Alfisol	3800-3000 (O-H stretch); 2300, 2260, 2290, 1500, 1400 (polymerization bands); 1648-1630 (H-O-H bond); 1600 (HA)	Minor attenuation in the 3800-3000 cm^{-1} region, less complexation. Peak around 1600 cm^{-1} stays intact	Lower complexation due to kaolinite-rich structure, minimal shift in functional groups
Inceptisol	3800-3000 (O-H stretch); 2300, 2260, 2290, 1500, 1400 (polymerization bands); 1648-1630 (H-O-H bond); 1080-917 (Al-OH)	Similar to Vertisol but less pronounced complexation. Shift in 3800-3000 cm^{-1} and 1648-1630 cm^{-1}	Strong interaction between clay and HA, especially in 3800-3000 cm^{-1} region
Entisol	3800-3000 (O-H stretch); 2300, 2260, 2290, 1500, 1400 (polymerization bands); 1648-1630 (H-O-H bond); 1080-917 (Al-OH)	Noticeable complexation with attenuation in 3800-3000 cm^{-1}; reduction in peaks around 1648-1630 cm^{-1}	Strong HA-clay interaction, significant shift in OH and C=C peaks

3.6 FTIR Spectra of Clay-Humus Complex

The FTIR spectra of clay and HA were compared, revealing a noteworthy diminution and attenuation in the clay-humus complex spectra (Fig.5). This attenuation signifies a robust association between HA and clay minerals. The complexation primarily involves the electrostatic, van der Waals, or hydrogen bonding interactions between octahedral hydroxyl (OH) groups in clay and OH groups in HA phenol/amine, resulting in a reduction and shift towards lower frequencies in the clay-humus complex FTIR spectra, particularly in the 3800-3000 cm^{-1} region. This phenomenon was notably pronounced in Vertisol, Inceptisol, and Entisol, while the least complexation was observed in the case of Alfisol. The assignments of various absorption peaks of clay-humus complex in different soil orders are shown in Table 7.

In all soil orders, specific peaks in the clay and HA spectra, such as those at 2300 cm-1, 2260 cm-1, 2290 cm-1, 1500 cm-1, and 1400 cm-1, exhibited a decrease in intensity and broadening in the clay-humus complexes. This alteration is attributed to the polymerization between clay and HA, indicating the formation of strong associations. Additionally, the peaks in the 1648-1630 cm-1 range, assigned to the strong hydrogen-oxygen-hydrogen (H-O-H) bonds of

absorbed water in hydrated phyllosilicate minerals, as well as aromatic C=C and C=O stretching in amide, ketone, and quinone groups of HAs, were strongly complexed and exhibited reduced intensity in Vertisol, Inceptisol, and Entisol. Conversely, in Alfisol, the strong hydrogen bonds of kaolinite-rich minerals remained unchanged, while the 1600 cm-1 peak in HA samples weakened after complexation in the clay-humus complex. This weakening indicates the involvement of ketones, carboxyl, and amide moieties in complexation with octahedral OH, while the unchanged 1600 cm-1 peak suggests that the strongly hydrogen-bonded O-H in the kaolinite-rich layer structure did not participate in complexation.

Furthermore, in the clay-humus complexes of all soil orders, the peak around 1080 to 917 cm^{-1}, associated with inner sphere aluminum hydroxyl (Al-OH) groups, exhibited a reduction, implying the active participation of organic moieties in the complexation process.

4. DISCUSSION

4.1 Stability of C in Clay-Humus Complexes of Different Soil Orders

The findings on the stability of C in clay-humus complexes across different soil orders of paddy

soil have significant implications for soil management practices focused on sustainable SOC retention. The variations in total C content and NaOCl-resistant C between soil types offer insights into which soil orders may provide long-term C storage, which is critical for soil health and climate mitigation strategies (Mukherjee, 2022). The total C content and NaOCl-resistant C enrichment serve as vital indicators, reflecting the persistence of SOC (Das et al., 2019). The observed variations in these features among different soil orders (Vertisol, Alfisol, Inceptisol, and Entisol) have been elucidated through a scientific lens. The elevated enrichment of NaOCl-resistant C in Vertisol, compared to other soil orders, may be attributed to the specific mechanisms of carbon protection facilitated by the presence of clay minerals in these soils (Das et al., 2019, Ahmed et al., 2002). Vertisol, characterized by a higher content of smectite, hydroxyl-interlayered minerals (HIMs), and smectite-rich interstratified clay minerals, exhibits a strong affinity for soil humus (Das et al., 2023, Jadhav et al., 2023). This affinity is corroborated by X-ray diffractogram analyses revealing the prevalence of these clay minerals in Vertisol. Studies by (Chotzen 2016, Kome et al. 2019) have previously noted the tendency of smectite-containing soils and sediments to harbor elevated organic matter. The permanence of negatively charged sites on smectite-rich minerals, resulting from isomorphic substitution, creates abundant active sites on clay mineral surfaces (Huang et al., 2024; Kumari and Mohan 2021). This phenomenon enhances the adsorption capacity of clay minerals for organic compounds, contributing to the higher total C and NaOCl-resistant C as observed in Vertisol.

In practice, this suggests Vertisols can be effectively managed for carbon sequestration with methods like conservation tillage or organic amendments, which take advantage of the high adsorption capacity of smectite-rich minerals (Chotzen, 2016; Kome et al., 2019). These approaches allow for increased C retention by enhancing the mineral-organic interactions facilitated by Vertisol's smectite content (Singh et al., 2017).

Conversely, the lower NaOCl-resistant C enrichment in Alfisol can be attributed to the predominance of kaolinite-rich minerals in these soils (Mikhail and James, 2015, Khan et al., 2023). Kaolinite is characterized by lower total surface area, minimal isomorphic substitution, and inaccessible interlayers for foreign

molecules, which hinders the humification of organic substances (Kumari and Mohan, 2021, Khan et al., 2023). As a result, in the present study, the total C and NaOCl-resistant C content in Alfisol is relatively low compared to other soil orders, signifying a lower C stability within the clay-humus complex. (Sukumaran et al., 2024, Purakayastha et al., 2019, Srinivasarao et al., 2009, Ahmed et al., 2002). So to improve C stability in Alfisols, strategies such as biochar application or cover cropping could be beneficial, as these added organic matter can help to increase SOC in kaolinite-dominant soils, where inherent C retention capacity is limited (Kumari and Mohan, 2021).

In Inceptisol and Entisol, the relatively higher NaOCl-resistant C content aligns with the prevalence of illite and illite-rich minerals. These minerals exhibit higher surface area and amphoteric properties on broken edges of clay minerals, facilitating greater retention of organic carbon (Kumari and Mohan, 2021; Khan et al., 2023). The observations presented by Wiseman and Puttmann, 2006 support the notion that illite-rich minerals contribute to enhanced C stability in these soil orders. For these soil orders, a balanced management approach involving periodic organic amendments, reduced tillage, and careful nutrient management can optimize C retention by leveraging illite's amphoteric sites for organic matter interactions (Kumari & Mohan, 2021; Khan et al., 2023). This is supported by the findings that illite-rich minerals enhance carbon stability in soil, especially where SOC sequestration is a goal (Barre et al., 2008; Datta et al., 2015).

Understanding these mineral-SOC interactions provides a framework for implementing tailored soil management practices to maximize SOC stabilization across diverse soil orders, directly supporting soil fertility, crop yield, and climate resilience (Das et al., 2019).

4.2 Elemental and Functional Characterization of Humic Acids

The reactivity of humic compounds in soil is usefully shown by its elemental composition. The most durable and widely dispersed organic material on the earth's surface is humic substances (Lehmann and Kleber, 2015; Goydaragh et al., 2021). The elemental composition of HA extracted from Vertisol recorded significantly higher values in the present study, due to intensive humification, a

greater degree of condensation of aromatic rings in Vertisol led to greater elemental carbon, nitrogen, and sulphur levels in humic materials than other soil orders (Tamfuh, 2011; Srinivasarao et al. (2009) So Vertisol's HA suggests strong carbon sequestration potential (Mohanty et al., 2020). Increased total acidity, due to carboxylic and phenolic-OH groups, enhances cation exchange capacity (CEC), making Vertisol ideal for reduced tillage and organic amendments to improve structure and nutrient retention (Srilatha et al., 2013). A low E4/E6 ratio indicates higher molecular weight HAs, signifying advanced humification and increased carbon stability under conservation practices (Ahmed et al., 2002, Reddy et al., 2018).Similar findings of Krishna and Mohan, 2017; Giweta, 2020 and Zhou et al., 2023 stated that the nature of OM (leaf litter, plant residues, FYM, organic manures etc.) added to the soil and its decomposition under various climates (dry and transitional heavy rainfall zones) has a significant influence on the elemental composition of humic substances. The index of functional groups (carboxylic and phenolic-OH groups) expressed as total acidity was significantly greater in Vertisol compared to Inceptisol, Alfisol and Entisol. Tamfuh (2011) and Srinivasarao et al. (2009) also observed similar results, attributing the variations in total acidity to inherent differences in the chemical composition and molecular weights of HAs. The E4/E6 ratio was significantly lower in Vertisol while higher in Entisol (Ahmed et al., 2002). Generally, the HAs with a ratio of < 5 serve as an index of humification and the ratio narrows with increasing molecular weight and condensation (Srilatha et al., 2013). A low E4/E6 ratio indicates higher molecular weight HAs, signifying advanced humification and increased carbon stability under conservation practices (Mathew et al., 2021; Jadhav et al., 2023). This is true for Entisol, where time is a limiting factor (Satisha and Devarajan, 2011; Tahiri et al., 2016).

4.3 FTIR spectroscopy of Humic Acid, Clay and Clay-Humus Complexes

HAs are probably the biggest single SOM pool in mineral soils (Banach-Szott and Tobiasova, 2021). The spectral characterization of HA, could reveal the importance of HA in carbon stability in different soil orders. Comparing all the HA and clay IR spectra of different soil orders, the clay-humus complexes IR spectra are reduced and have lower peaks (Ampee, 2018; Singh et al., 2016). This indicates that strong bonding

between humic substances and the layer silicate minerals (Ampee, 2018; Suman et al.,2020; Nuzzo et al., 2020).

Vertisol and Inceptisol's HA, clay and clay humus complex spectra have similar absorption peaks. The HA spectra of these soil orders have intense and sharp peaks of aromatic C=C and C=O in amide, ketone, and quinone stretching and reduced and weak peaks of aliphatic C-H stretching which indicates that a higher percentage of aromatic C due to the advanced stage of humification, the concentration of recalcitrant organic compounds increased and tends toward higher aromaticity (Giovanela et al., 2010). Absorption caused by aliphatic C-H stretching varied considerably, being strong in Vertisol, Inceptisol but not in Entisol and Alfisol (Ampee, 2018). The absence of pronounced peaks in this region may be due to the extensive substitution of aromatic ring or masking from the broad band resulting from OH stretching (Giovanela et al.,2010; Zhang et al.,2016; Pärnpuu et al., 2022.). This can also be concluded with the support of the IR spectra of clay. In IR spectra of Vertisol and Inceptisol indicated the dominance of smectite and smectite rich minerals which have greater surface area for adsorption and higher layer charge than other silicate layer minerals this led the way for higher affinity towards the organic matter (Sukumaran et al. 2024, Das et al., 2019). The organic matter fixed within the interlayer of these hydrated phyllosilicates represented the stable carbon resistant to degradation and underwent a humification process which showed higher aromaticity in these soil orders (Xu et al., 2024). In IR spectra of Vertisol and Inceptisol clay samples, the peak around 1600 cm^{-1} remains unchanged but in HA samples became weak after complexation. This suggests that aromatic carbon groups (C=C and C=O), along with ketones, carboxyl, and amide groups, form weak complexes with octahedral OH, resulting in weak or reduced peaks in the HA spectra. However, the strong hydrogen-bonded O-H in the silicate clay layer structure remains unchanged, indicating it does not participate in the complexation (Ahmed et al., 2002; Das et al., 2019; Ampee, 2018). The IR spectra of Entisol indicated the presence of illite, kaolinite, and smectite type clay minerals which show an average stability of C in these soils as compared to Alfisol (Ahmed et al., 2002). The IR spectra of Alfisol clay showed the presences of kaolinite and kaolinite rich minerals which has a lower total surface area and its interlayers are not

accessible by foreign molecules, leading to very slow humification process in these soil orders. The same can be proved by the IR spectra of Alfisol clay humus complex, where the clay-HA linkage is probably through hydrogen or other monovalent cation bridges which is generally very weak in nature causing lower carbon stability (Das et al., 2019). Ahmed et al. (2002) also reported that Alfisol has weakest clay-HA bonding compared to Vertisol, Mollisol and Entisol.

The stronger bonding observed in Vertisol and Inceptisol, can be attributed to higher aromaticity and recalcitrant organic compounds, leading to enhanced carbon sequestration potential (Jha et al., 2012; Kaushal et al., 2023). Management practices in Vertisol and Inceptisol, like reduced tillage and organic amendments could further boost carbon stability in Vertisol and Inceptisol by enhancing organic matter interactions within clay minerals. (Pal and Pal, 2017; Das et al., 2019). Practices like increasing organic inputs or addition of soil amendments that promote C stabilization such as adding compost, manure, crop residues, practicing reduced tillage, and integrating agroforestry, may compensate for this lower intrinsic carbon stability (Ampee, 2018; Das et al., 2022; Naik et al., 2023). These recommendations align with previous research which indicates that targeted organic additions can improve C retention, particularly in soils with low clay-HA complex stability, like Alfisol (Ahmed et al., 2002).

In summary, the study underscores that enhancing carbon stability in soils may require tailored management based on soil mineralogy, where Vertisol and Inceptisol benefit from practices that leverage strong HA-clay interactions, while Alfisol may need amendments to enhance organic matter stabilization.

5. CONCLUSION

Variations in clay mineralogy among soil types significantly influence carbon stability in clay-humus complexes. Vertisol, rich in smectite, exhibits the highest carbon stability, while Alfisol, dominated by kaolinite, shows lower stability. The content of NaOCl-resistant carbon reflects this trend, underscoring the role of clay minerals in carbon sequestration. Elemental and functional analyses of HAs support these findings, with Vertisol supporting advanced humification. FTIR spectroscopy highlights strong

complexation in Vertisol, Inceptisol, and Entisol, emphasizing effective carbon stabilization through mineral interactions, especially in soils with higher smectite content. This study underscores the crucial role of soil mineralogy, particularly clay composition, in influencing carbon stability across different soil orders. The insights gained from mineralogical, elemental, and spectroscopic analyses enhance our understanding of SOC dynamics, providing a scientific basis for soil management practices aimed at improving carbon sequestration and overall soil health. The future research could delve deeper into understanding the mechanisms of clay-organic interactions under different climate and management scenarios, particularly focusing on soils with lower natural carbon stability, such as Alfisols.

DISCLAIMER (ARTIFICIAL INTELLIGENCE)

Author(s) hereby declares that NO generative AI technologies such as Large Language Models (ChatGPT, COPILOT, etc.) and text-to-image generators have been used during the writing or editing of this manuscript.

COMPETING INTERESTS

Authors have declared that no competing interests exist.

REFERENCES

Ahmed, N., Varadachari, C., & Ghosh, K. (2002). Soil clay-humus complexes II: Bridging cations and DTA studies. *Australian Soil Research, 40*(5), 705-713.

Ampee, T. (2018). *Clay humus stability under different land use systems and its impact on nutrient availability in soils of Siang districts of Arunachal Pradesh* (Ph.D. dissertation). Indian Agricultural Research Institute, New Delhi, India.

Banach-Szott, M., Debska, B., & Tobiasova, E. (2021). Properties of humic acids depending on the land use in different parts of Slovakia. *Environmental Science and Pollution Research, 28*(48), 58068-58080.

Barre, P., Velde, B., Fontaine, C., Catel, N., & Abbadle, L. (2008). Which 2:1 clay minerals are involved in the soil potassium reservoir? Insights from potassium addition or removal experiments on three

temperate grassland soil clay assemblages. *Geoderma, 146*(1-2), 216-223.

Bottone, A., Boily, J. F., Shchukarev, A., Andersson, P. L., & Klaminder, J. (2022). Sodium hypochlorite as an oxidizing agent for the removal of soil organic matter before microplastics analyses. *Journal of Soils and Sediments, 51*, 112-122.

Chotzen, R., Polubesova, T., Chefetz, B., & Mishael, Y. (2016). Adsorption of soil-derived humic acid by seven clay minerals: A systematic study. *Clays and Clay Minerals, 64*(6), 628-638.

Das, A., Purakayastha, T. J., Ahmed, N., Das, R., Biswas, S., Shivay, Y. S., Sehgal, V. K., Rani, K., Trivedi, A., Tigga, P., & Sahoo, J. (2023). Influence of clay mineralogy on soil organic carbon stabilization under tropical climate, India. *Journal of Soil Science and Plant Nutrition, 23*(4), 1003-1018.

Das, R., Purakayastha, T. J., Das, D., Ahmed, N., Kumar, R., Biswas, S., Walia, S. S., Singh, R., Shukla, V. K., Yadava, M. S., Ravisankar, N., & Datta, S. C. (2019). Long-term fertilization and manuring with different organics alter the stability of carbon in colloidal organo-mineral fraction in soils of varying clay mineralogy. *Science of the Total Environment, 684*, 682-693.

Das, T. K., Saharawat, Y. S., Bhattacharyya, R., Sudhishri, S., Bandyopadhyay, K. K., Sharma, A. R., & Jat, M. L. (2018). Conservation agriculture effects on crop and water productivity, profitability, and soil organic carbon accumulation under a maize-wheat cropping system in the Northwestern Indo-Gangetic Plains. *Field Crops Research, 215*, 222-231.

Datta, S. C., Takkar, N. K., & Verma, U. K. (2015). Assessing stability of humus in soils from continuous rice-wheat and maize-wheat cropping systems using kinetics of humus desorption. *Communications in Soil Science and Plant Analysis, 46*(23), 2888-2900.

Giovanela, M., Crespo, J. S., Antunes, M., Adametti, D. S., & Fernandes, A. N. (2010). Chemical and spectroscopic characterization of humic acids extracted from the bottom sediments of a Brazilian subtropical microbasin. *Journal of Molecular Structure, 981*(1-3), 111-119.

Giweta, M. (2020). Role of litter production and its decomposition and factors affecting the processes in a tropical forest ecosystem: A review. *Journal of Ecology and Environment, 44*(1), 11-17.

Goydaragh, M. G., Taghizadeh-Mehrjardi, R., Jafarzadeh, A. A., Triantafilis, J., & Lado, M. (2021). Using environmental variables and Fourier Transform Infrared Spectroscopy to predict soil organic carbon. *Catena, 202*, 105280.

Huang, R., Wu, L., Wang, X., Tang, N., Gao, L., Wang, A., & Lu, Y. (2024). Review on the effect of isomorphic replacement on the structure and application performance of typical clay minerals. *Progress in Natural Science*, 112-119.

Jackson, M. L. (1985). *Soil chemical analysis: Advanced course* (2nd ed.). University of Wisconsin, Madison.

Jadhav, K. P., Ahmed, N., Datta, S. P., Das, R., Ray, P., Meena, M. C., Chakraborty, D., & Shrivastava, M. (2023). Chemical and instrumental characterization of humic acid of diverse soil orders under paddy cultivation. *Environment and Ecology, 41*, 38-44.

Jagadamma, S., Lal, R., Ussiri, D. A., Trumbore, S. E., & Mestelan, S. (2010). Evaluation of structural chemistry and isotopic signatures of refractory soil organic carbon fraction isolated by wet oxidation methods. *Biogeochemistry, 98*(1), 29-44.

Jha, P., Biswas, A. K., & Rao, A. S. (2012). Carbon sequestration in agricultural soils: Evolving concepts, issues, and strategies. In *Carbon management in agriculture for mitigating greenhouse effect* (pp. 17-26). ICAR Research Complex for NEH Region, Umiam, Meghalaya, India.

Kaushal, S., Sharma, N., Singh, I., & Singh, H. (2023). Soil carbon sequestration: A step towards sustainability. *International Journal of Plant & Soil Science, 35*(11), 160-171.

Khan, S., Ajmal, S., & Hussain, T. (2023). Clay-based materials for enhanced water treatment: Adsorption mechanisms, challenges, and future directions. *Journal of Umm Al-Qura University for Applied Sciences, 56*, 76-80.

Kome, G. K., Enang, R. K., Tabi, F. O., & Yerima, B. P. K. (2019). Influence of clay minerals on some soil fertility attributes: A

review. *Open Journal of Soil Science, 9*, 155-188.

Krishna, M. P., & Mohan, M. (2017). Litter decomposition in forest ecosystems: A review. *Energy, Ecology and Environment, 2*(3), 236-249.

Kumar, D., Purakayastha, T. J., Das, R., Yadav, R. K., Shivay, Y. S., Jha, P. K., Singh, S., Aditi, K., & Prasad, P. V. V. (2022). Long-term effects of organic amendments on carbon stability in clay-organic complex and its role in soil aggregation. *Agronomy, 13*(1), 39.

Kumari, N., & Mohan, C. (2021). Basics of clay minerals and their characteristic properties. *Clay Science, 24*, 13-16.

Kundu, S., Srinivasarao, C., Reddy, K. S., Prasad, J. V. N. S., Indoria, A. K., Veni, V. G., & Singh, V. K. (2022). Soil carbon management in rainfed production systems. *Indian Farming, 72*(11), 54-57.

Lal, R., Bouma, J., Brevik, E., Dawson, L., Field, D. J., Glaser, B., Hatano, R., Hartemink, A. E., Kosaki, T., Lascelles, B., & Monger, C. (2021). Soils and sustainable development goals of the United Nations: An International Union of Soil Sciences perspective. *Geoderma Regional, 25*, e00398.

Lawrence, C., Harden, J., Xu, X., Schulz, M., & Trumbore, S. (2015). Long-term controls on soil organic carbon with depth and time: A case study from the Cowlitz River Chronosequence, WA, USA. *Geoderma, 247*, 23-30.

Lehmann, J., & Kleber, M. (2015). The contentious nature of soil organic matter. *Nature, 528*(7580), 60-68.

Lutzow, M., Kogel-Knabner, I., Matzner, E., Guggenberger, G., Marschner, B. H., & Flessa, H. (2009). Stabilization of organic matter in temperate soils: Mechanisms and their relevance under different soil conditions—a review. *European Journal of Soil Science, 57*(4), 426-445.

Mabagala, F. S. (2022). On the tropical soils: The influence of organic matter (OM) on phosphate bioavailability. *Saudi Journal of Biological Sciences, 29*(6), 3635-3641.

Mathew, J., Gopinath, A., & Vareed, R. A. (2021). Spectroscopic characterization of humic substances isolated from tropical mangrove sediments. *Arabian Journal of Geosciences, 14*(3), 1-15.

Mikhail, B., & James, D. (2015). Adsorption of inorganic and organic solutes by clay minerals. In *Clay Minerals: Properties, Applications and Environmental Issues* (pp. 24-33). Elsevier.

Mohanty, M., Sinha, N. K., Somasundaram, J., McDermid, S. S., Patra, A. K., Singh, M., Dwivedi, A. K., Reddy, K. S., Rao, C. S., Prabhakar, M., & Hati, K. M. (2020). Soil carbon sequestration potential in a Vertisol in central India: Results from a 43-year long-term experiment and APSIM modeling. *Agricultural Systems, 184*, 102906.

Mukherjee, S. (2022). Soil carbon sequestration. In *Current Topics in Soil Science: An Environmental Approach* (pp. 233-239). Cham: Springer International Publishing.

Naik, B. S., Reddy, G. P., Yadav, S. K., Sharma, S. K., Choudhary, R., & Choudhary, P. (2021). Carbon sequestration: The great opportunity of a challenging task in soil. *Current Research in Agricultural Sciences, 2*(1), 23-41.

Naresh, R. K., Singh, S. P., Gupta, R. K., et al. (2018). Long-term effects of tillage and residue management on soil aggregation, soil carbon sequestration, and energy relations under a rice-wheat cropping system in typic ustochrept soil of Uttar Pradesh. *Journal of Pharmacognosy and Phytochemistry, 7*(1), 237-247.

Nuzzo, A., Buurman, P., & Cozzolino, V. (2020). Infrared spectra of soil organic matter under a primary vegetation sequence. *Chemical Biology and Technology in Agriculture, 7*(1), 6-9.

Pärnpuu, S., Astover, A., Tõnutare, T., Penu, P., & Kauer, K. (2022). Soil organic matter qualification with FTIR spectroscopy under different soil types in Estonia. *Geoderma Regional, 28*, e00483.

Purakayastha, T. J., Das, R., Kumari, S., Shivay, Y. S., Biswas, S., Kumar, D., & Chakrabarti, B. (2019). Impact of continuous organic manuring on mechanisms and processes of the stabilization of soil organic carbon under rice-wheat cropping system. *Soil Research, 22*(1), 73-83.

Rashid, M., Qaiser, H., Rifat, H., Ahmed, M., Riaz, M., Khan, K. S., Muhammad, I. A., Sarosh, A. A., & Khalid, B. (2022). Soil carbon and legumes. In *Advances in*

Legumes for Sustainable Intensification (pp. 329). Elsevier.

Reddy, S. B., Nagaraja, M. S., Kadalli, G. G., & Champa, B. V. (2018). Fourier transform infrared (FTIR) spectroscopy of soil humic and fulvic acids extracted from paddy land use system. *International Journal of Current Microbiology and Applied Sciences, 7*(5), 834-837.

Rout, K. K., Shirale, S. T., & Rajani, A. V. (2024). Assessment of carbon carrying capacities of Alfisols and Vertisols under long-term manuring and fertilization. *Soil and Tillage Research, 238*, 105994.

Sarkar, B., Singh, M., Mandal, S., Churchman, G. J., & Bolan, N. S. (2018). Clay minerals—Organic matter interactions in relation to carbon stabilization in soils. In *The Future of Soil Carbon* (pp. 71-86). Academic Press.

Satisha, G. C., & Devarajan, L. (2011). Composition and characterization of humic substances extracted from effluent-based pressmud composts. *Agropedology, 21*(1), 8-17.

Schnitzer, M., & Gupta, U. C. (1965). Determination of acidity in soil organic matter. *Soil Science Society of America Proceedings, 29*(3), 274-277.

Schweizer, S. A., Mueller, C. W., Höschen, C., Ivanov, P., & Kögel-Knabner, I. (2021). The role of clay content and mineral surface area for soil organic carbon storage in an arable toposequence. *Biogeochemistry, 156*(3), 401-420.

Singh, B., Fang, Y., & Johnston, C. T. (2016). A Fourier-transform infrared study of biochar aging in soils. *Soil Science Society of America Journal, 80*(3), 613-622.

Singh, M., Sarkar, B., Biswas, B., Bolan, N. S., & Churchman, G. J. (2017). Relationship between soil clay mineralogy and carbon protection capacity as influenced by temperature and moisture. *Soil Biology and Biochemistry, 109*, 95-106.

Singh, V. K., Kundu, S., & Naveen, J. (2023). Soil carbon management for a sustainable food system. *Indian Farming, 73*(6), 25-29.

Srilatha, M., Rao, P. C., Sharma, S. H. K., & Padmaja. (2013). Physico-chemical characterization of humic substances under long-term application of fertilizers and manures in rice-rice cropping sequence in an Inceptisol. *International Journal of Advanced Research, 1*(10), 343-348.

Srinivasarao, C., Vittal, K. P. R., Venkateswarlu, B., Wani, S. P., Sahrawat, K. L., Marimuthu, S., & Kundu, S. (2009). Carbon stocks in different soil types under diverse rainfed production systems in tropical India. *Communications in Soil Science and Plant Analysis, 40*(23), 2338-2356.

Stevenson, F. J. (1994). *Humus Chemistry: Genesis, Composition, Reactions* (2nd ed.). Wiley.

Stoner, S., Trumbore, S. E., González-Pérez, J. A., Schrumpf, M., Sierra, C. A., Hoyt, A. M., Chadwick, O., & Doetterl, S. (2023). Relating mineral–organic matter stabilization mechanisms to carbon quality and age distributions using ramped thermal analysis. *Philosophical Transactions of the Royal Society A, 381*(2210), 20230139.

Sukumaran, S., Purakayastha, T. J., Sarkar, B., Chakrabarti, B., Bandyopadhyay, K. K., Kumar, D., Yadav, R. K., & Viswanath, T. (2024). Assessment of carbon carrying capacities of Alfisols and Vertisols under long-term manuring and fertilization. *Soil and Tillage Research, 238*, 105994.

Tahiri, A., Richel, A., Destain, J., Druart, P., Thonart, P., & Ongena, M. (2016). Comprehensive comparison of the chemical and structural characterization of landfill leachate and leonardite humic fractions. *Analytical and Bioanalytical Chemistry, 408*(7), 1917-1928.

Tamfuh, A. P., Emmanuel, D., Bitom, W., Njopwouo, D., & Daniel. (2011). Petrological, physico-chemical, and mechanical characterization of the topomorphic Vertisols from the Sudano-Sahelian region of North Cameroon. *Open Geology Journal, 5*, 14-21.

Wiseman, C. L. S., & Puttmann, W. (2006). Interactions between mineral phases in the preservation of soil organic matter. *Geoderma, 134*(1-2), 109-118.

Xu, Z., & Tsang, D. C. W. (2024). Mineral-mediated stability of organic carbon in soil and relevant interaction mechanisms. *Eco-Environmental Health, 3*(1), 59-76.

Yang, J. Q., Zhang, X., Bourg, I. C., & Stone, H. (2021). 4D imaging reveals mechanisms of clay-carbon protection and release. *Nature Communications, 12*(1), 622.

Zhang, Z. Y., Huang, L., Liu, F., Wang, M. K., Fu, Q. L., & Zhu, J. (2016). Characteristics of clay minerals in soil particles of two Alfisols in China. *Applied Clay Science, 120*, 51-60.

Zhou, X., Kun, D., Tang, Y., Huang, H., Peng, G., & Wang, D. (2023). Research progress on the decomposition process of plant litter in wetlands: A review. *Water, 18*(3), 3246. https://doi.org/10.3390/w1518324

Peer-review history:
The peer review history for this paper can be accessed here:
https://www.sdiarticle5.com/review-history/126719